

Measurement of evaporation-residue cross sections with light beams and deformed lanthanide target nuclei

著者	Ueno Shingo, Toda Kaoru, Asano A., Takahashi Naruto, Kasamatsu Y., Yokokita T., Yokoyama Akihiko
journal or publication title	Journal of Radioanalytical and Nuclear Chemistry
volume	303
number	2
page range	1273-1276
year	2014-01-01
URL	http://hdl.handle.net/2297/40162

doi: 10.1007/s10967-014-3632-x

Title – Measurement of evaporation-residue cross sections with light beams and deformed lanthanide target nuclei

Names - S. Ueno¹, K. Toda¹, A. Asano¹, N. Takahashi², Y. Kasamatsu², T. Yokokita², A. Yokoyama³

Affiliations – ¹Graduate School of Natural Science and Technology, Kanazawa University, Kakuma, Kanazawa, Ishikawa 920-1192, Japan, ²Graduate School of Science, Osaka University, Toyonaka, Osaka 560-0043, Japan, ³Institute of Science and Engineering, Kanazawa University, Kakuma, Ishikawa, Kanazawa 920-1192, Japan

Corresponding author –

S. Ueno, 076-264-5746, coffeepudding1126@yahoo.co.jp

Abstract – To obtain a better understanding of the fusion reaction, we have focused on reactions involving deformed nuclei. Evaporation residue cross sections of the $^{169}\text{Tm}+^{20}\text{Ne}$ reaction were measured, from which we extracted the fusion excitation function. This is compared with literature data of the $^{169}\text{Tm}+^{16}\text{O}$ and $^{165}\text{Ho}+^{20}\text{Ne}$ systems. Irradiation with ^{20}Ne ion beam has been carried out at the incident energy near the Coulomb barrier, where the effect of nuclear deformation is prominent. The results are consistent with the idea that the degree of deformation has an effect on the threshold value of the excitation functions near the Coulomb barrier.

Keywords – Fusion reaction/ Excitation function/ Deformed nucleus/
HIVAP code

Introduction

Production of superheavy nuclei is one of the most worthwhile works in nuclear physics and nuclear chemistry to identify the location of closed shell structures in the extreme region of the chart of nuclei as well as to investigate the atomic properties [1—3]. A good understanding of the fusion process is important for reliable estimates of cross sections for the production of superheavy nuclei. In heavy-ion induced reactions, to examine precisely the evaporation residue cross section is difficult if fission is the main reaction exit channel. Measurement of the evaporation residue cross sections is important because it gives information not only on the fusion probability but also on the following particle evaporation. It is worth-while to study the evaporation residue production from non-fissile compound nuclei to understand the reaction mechanism as a simulation of production of superheavy nuclei.

We have focused on the influence of the deformation of target nuclei on the fusion cross section because the nuclei of actinides used as target nuclei for superheavy element production via hot fusion reactions are deformed.

In this study, in order to investigate the effect of the degree of nuclear deformation on the fusion reaction, we have studied the cross sections of evaporation residues directly from $xn/pxn/\alpha xn$ channels or

their beta-decay in the nuclear reaction $^{169}\text{Tm}+^{20}\text{Ne} \rightarrow ^{189}\text{Au}^*$ at energies near the Coulomb barrier and compared the results with those of $^{169}\text{Tm}+^{16}\text{O} \rightarrow ^{185}\text{Ir}^*$ [4] and $^{165}\text{Ho}+^{20}\text{Ne} \rightarrow ^{185}\text{Ir}^*$ [5] reactions. The lanthanoid nuclei used as the targets in those reactions are deformed as well as actinides and they hardly lead to fission in the nuclear reaction.

The deformation of nuclei is related to the electric quadrupole moment (Q). The value of Q/e of ^{20}Ne , ^{16}O , ^{169}Tm and ^{165}Ho is -0.23, 0, -1.2 and 3.58 b [7]. The deformation of nuclei are estimated with the values of Q by Eq.1,

$$\frac{Q}{e} = \frac{2}{5}Z(a^2 - b^2) \text{ (b)}, \quad (1)$$

where e is the elementary charge, Z , the atomic number, a , the half-length of a spheroid along the rotation axis direction and b , its half-length along the axis perpendicular to the rotational axis in the spheroid approximation.

The corresponding degree of the deformation (a/b) of ^{20}Ne , ^{16}O , ^{169}Tm and ^{165}Ho is 0.75, 1, 0.95 and 1.16 if the nuclear radius parameter is 1.2 fm. In the $^{169}\text{Tm}+^{20}\text{Ne}$ and $^{165}\text{Ho}+^{20}\text{Ne}$ systems, the target nucleus ^{165}Ho is more deformed than ^{169}Tm . In the $^{169}\text{Tm}+^{16}\text{O}$ and $^{169}\text{Tm}+^{20}\text{Ne}$ systems, the projectile nucleus ^{16}O is spherical, while ^{20}Ne is deformed. From a comparison of the results, we can extract the effect of nuclear deformation. Besides, we compare the systems of $^{169}\text{Tm}+^{16}\text{O}$ and $^{165}\text{Ho}+^{20}\text{Ne}$ forming the same compound nucleus, $^{185}\text{Ir}^*$ and can thus examine the effect of the entrance channel for the

systems. From a comparison of the results, we can learn about the effect of nuclear deformation.

Experimental

The bombardment for synthesis of the heavy nuclei was carried out using a ^{20}Ne beam supplied from the AVF cyclotron at Research Center for Nuclear Physics (RCNP), Osaka University, Japan. The targets were prepared by electrodeposition with a standard solution of $^{\text{nat}}\text{Tm}$ on an Al foil of 2.7 mg/cm^2 in thickness. This foil was also served as a catcher foil. The ^{169}Tm content was $4.5\text{-}5.1 \text{ mg/cm}^2$ in the targets.

In order to cover a wide energy range in a single irradiation, the energy degradation technique was used. In the present experiment, two stacks with four targets each were prepared and each stack was irradiated at a different energy below 155 MeV. Typical beam intensity of ^{20}Ne was $1 \text{ particle-}\mu\text{A}$. A Faraday cup was used to measure the integrated beam current. The radioactivities produced in each target were assayed by γ -ray spectrometry using a high resolution HPGe detector.

In order to determine the production cross section of these residues, the residues were identified with the energies of characteristic γ -radiations and half-lives given in Table 1, along with the data taken from [6, 7]. The observed nuclides are either produced as beta-decay products of xn evaporation channel residues or directly in charged particle evaporation channels. The uncertainties of the cross sections include that from target atom number and that from the counting

statistics. Otherwise, the uncertainty of the beam dose is estimated to be around 5%.

Results and discussion

The evaporation residues detected in the $^{169}\text{Tm}+^{20}\text{Ne}$ system were ^{185}gPt , $^{183-185}\text{Ir}$, $^{181-183}\text{Os}$ and ^{181}Re . Most of the residues are supposed to be produced in the $(^{20}\text{Ne}, xn)$ reactions and some of them are decay products of the precursors. Figs. 1 and 2 shows the excitation functions for fusion reaction of $^{169}\text{Tm}+^{20}\text{Ne}$ compared with the theoretical calculations using the HIVAP code [8]. The HIVAP code is used for a theoretical calculation taking into consideration the degree of deformation of the nuclei and often used for estimation of production for superheavy nuclei. In Fig. 1, excitation functions are shown for each mass number of the products to assure the identification from γ -ray peaks. Dominant production energies of the nuclides are reproduced by the calculation, although absolute values of some cross sections are shifted from the calculation values. The cross sections are summed up to construct the total fusion excitation function in the $^{169}\text{Tm}+^{20}\text{Ne}$ system in Fig. 2. For the cross sections for two lowest energies, their upper limits are estimated from the upper cross sections of unobserved nuclides, and their lower limits are from those of observed nuclides. The calculation overestimates the experimental cross section in the higher energy region at $E_{\text{cm}} > 95$ MeV. On the other hand, sub-barrier data is closer to the calculation taking into account the deformation of ^{169}Tm and ^{20}Ne . However, as the attenuation of the

beam energy through the targets at the lowest energy is so large, it is difficult to assert the influence of deformation of the nucleus on fusion reaction from the data.

In Fig. 3, the experimental excitation functions for the fusion reactions $^{169}\text{Tm}+^{20}\text{Ne}$, $^{169}\text{Tm}+^{16}\text{O}$ [4] and $^{165}\text{Ho}+^{20}\text{Ne}$ [5] along with the calculated values for these systems are shown. In order to compare the systems among different entrance channels, we let the difference between the center-of-mass energy (E_{cm}) and the Coulomb barrier (B_c) [9] ($E_{\text{cm}} - B_c$), be the horizontal axis in the figure. For both systems of $^{169}\text{Tm}+^{20}\text{Ne}$ and $^{165}\text{Ho}+^{20}\text{Ne}$, the threshold energies for fusion were found to be close to each other. The result is consistent with the HIVAP calculations. On the other hand, comparing the systems $^{169}\text{Tm}+^{16}\text{O}$ and $^{169}\text{Tm}+^{20}\text{Ne}$, the latter, with the more deformed projectile of ^{20}Ne already fuses at lower incident energy. Further, comparing the systems $^{169}\text{Tm}+^{16}\text{O}$ and $^{165}\text{Ho}+^{20}\text{Ne}$, the latter system, where both partners are more deformed, starts to fuse at lower incident energy, even though the same compound nucleus is formed. As for the influence of the deformation of nuclei on the fusion cross sections near the Coulomb barrier, a similar observation was reported by D.J. Hinde et al. [10] for the $^{238}\text{U}+^{16}\text{O}$ system.

Conclusions

In this work, in order to investigate the effect of the degree of nuclear deformation on the fusion reaction, we have studied the fusion reaction $^{169}\text{Tm}+^{20}\text{Ne}$, and compared this system to $^{169}\text{Tm}+^{16}\text{O}$ [4] and

$^{165}\text{Ho}+^{20}\text{Ne}$ [5] in the energy region near the Coulomb barrier. The comparison of each experimental system yields that the results are consisted with the idea that the degree of deformation influences the rising edge of the excitation functions near the Coulomb barrier.

Acknowledgements

The authors thank the crew of RCNP for the beam operation and K. Nishio of JAEA for carrying out the calculation of excitation functions of experimental systems.

References

- [1]Oganessian Yu Ts (2007) Heaviest nuclear from ^{48}Ca -induced reactions. J Phys G 34:165-242
- [2]Hofmann S, Münzenberg G (2000) The discovery of the heaviest elements. Rev Mod Phys 72:733-767
- [3]Morita K, Morimoto K, Kaji D, Akiyama T, Goto S, Haba H, Ideguchi E, Kanungo R, Katori K, Koura H, Kubo H, Ohnishi T, Ozawa A, Suda T, Sueki K, Xu H, Yamaguchi T, Yoneda A, Yoshida A, Zhao Y (2004) Experimental on the Synthesis of Element 113 in the Reaction $^{209}\text{Bi}(^{70}\text{Zn}, n)^{278}113$. J Phys Soc Jpn 73:2593-2596
- [4]Asano A, Kaiya H, Araki M, Nishikawa M, Ooe K, Kikunaga H, Takahashi N, Yokoyama A (2009) Nuclear deformation effect on the excitation function of heavy ion fusion reaction on rare earth targets with the O-16 projectile. J Nucl Rad Sci 10:127

- [5] Toda K, Ueno S, Takahashi N, Kasamatsu Y, Yokokita T, Ooe K, Yokoyama A (2012) Excitation Functions for Fusion Reaction with Projectiles of Different Deformation. *J Nucl Rad Sci* 13:93
- [6] Reus U, Westmeier W (1983) CATALOG OF GAMMA RAYS FROM RADIOACTIVE DECAY Part 1 and 2. Springer-Verlag, United States
- [7] Firestone R B, (1996) Table of Isotopes 8th edition Volume 2. Wiley, New York
- [8] Reisdorf W, Schädel M (1992) How well do we understand the synthesis of heavy elements by heavy-ion induced fusion?. *Z Phys A* 343:47-57
- [9] Bass R (1980) Nuclear Reactions with Heavy Ions. Springer-Verlag, New York
- [10] Hinde D J, Dasgupta M, Leigh J R, Lestone J P, Mein J C, Morton C R, Newton J O, Timmers H (1995) Fusion-Fission versus Quasifission: Effect of Nuclear Orientation. *Phys Rev Lett* 74:1295-1298

Table 1 List of identified evaporation residues in the $^{169}\text{Tm}+^{20}\text{Ne}$ system with their spectroscopic properties and production channels. [6]

Residue	$T_{1/2}$	E_{γ} (keV)	I_{γ} (%)	Main channels	Other channels
$^{185\text{g}}\text{Pt}$	1.2 h	135.3	80	$4\text{n}+\beta^+$	$\text{p}3\text{n}$
		197.4	74		
		229.6	100		
^{185}Ir	14.4 h	254.3	13	$4\text{n}+2\beta^+$	$\text{p}3\text{n}+\beta^+$
^{184}Ir	3.0 h	264.0	67.5	$5\text{n}+2\beta^+$	αn
		390.4	25.7	$\text{p}4\text{n}+\beta^+$	
^{183}Ir	55 m	282.4	70	$6\text{n}+2\beta^+$	$\alpha 2\text{n}$
				$\text{p}5\text{n}+\beta^+$	
$^{183\text{m}}\text{Os}$	9.9 h	1102.0	50	$6\text{n}+3\beta^+$	$\alpha 2\text{n}+\beta^+$
		1108.0	23	$\text{p}5\text{n}+2\beta^+$	
$^{183\text{g}}\text{Os}$	13.0 h	114.4	20.8	$6\text{n}+3\beta^+$	$\alpha 2\text{n}+\beta^+$
		381.7	77.0	$\text{p}5\text{n}+2\beta^+$	
^{182}Os	22.1 h	180.2	36.8	$7\text{n}+3\beta^+$	$\alpha 3\text{n}+\beta^+$
				$\text{p}6\text{n}+2\beta^+$	
$^{181\text{g}}\text{Os}$	1.8 h	238.8	45.8	$8\text{n}+3\beta^+$	$\alpha 4\text{n}+\beta^+$
		827.0	20.8	$\text{p}7\text{n}+2\beta^+$	
^{181}Re	20 h	360.7	12.0	$8\text{n}+4\beta^+$	$\alpha 4\text{n}+2\beta^+$
		365.5	56.4	$\text{p}7\text{n}+3\beta^+$	

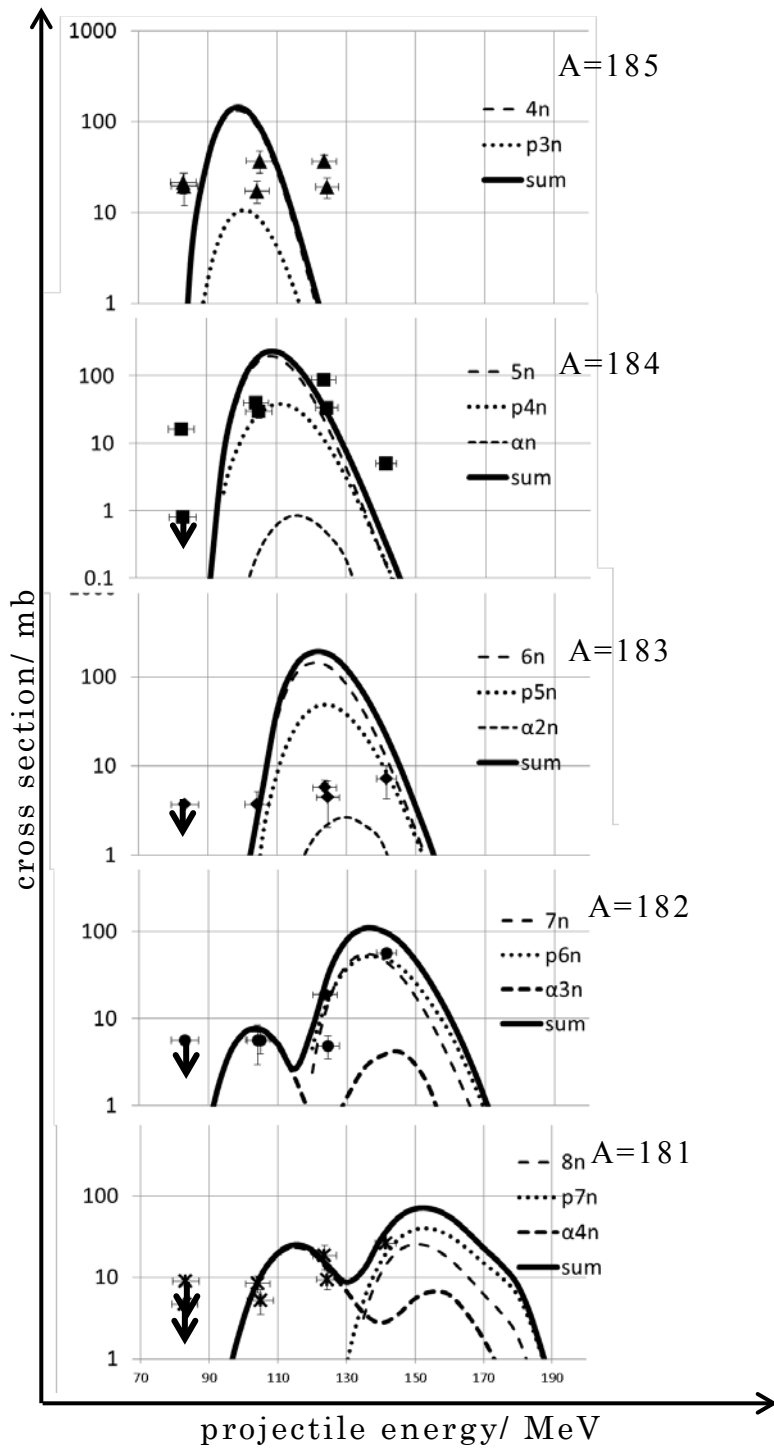


Figure 1 Excitation functions for each exit channel.

Solid curves are calculated with HIVAP taking into account the deformation of ^{169}Tm . Down arrows represent the upper limits of the cross sections.

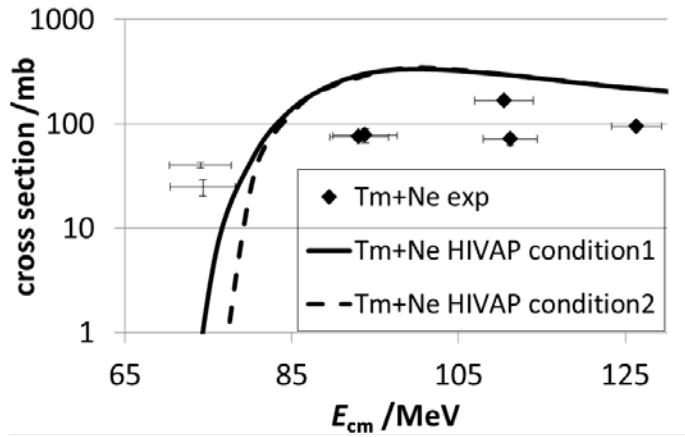


Figure 2 Excitation functions for the fusion reaction of $^{169}\text{Tm} + ^{20}\text{Ne}$ and calculated values with the code HIVAP. Solid and dashed curves represent the HIVAP calculations with (condition 1) and without (condition 2) taking into account the deformation of ^{169}Tm . Two marks at the lowest energy represent the range with the upper and lower limits.

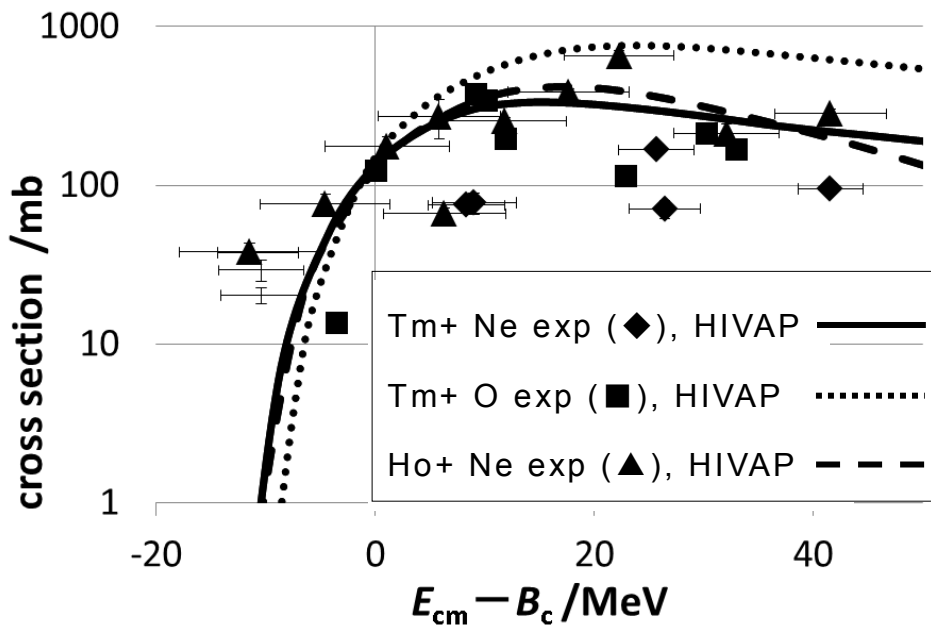


Figure 3 Excitation functions of $^{169}\text{Tm} + ^{20}\text{Ne}$ (\blacklozenge , closed rhombuses), $^{169}\text{Tm} + ^{16}\text{O}$ (\blacksquare , closed squares) [4] and $^{165}\text{Ho} + ^{20}\text{Ne}$ (\blacktriangle , closed triangles) [5] compared to theoretical values for the same systems.